PHYSICAL REVIEW B **78**, 144108 (2008)

Significant softening of c_{66} and hidden order parameter in the magnetic ordered state of $La_{2-x}Ca_xCoO_4$ $(0.4 \leq x \leq 0.7)$

K. Horigane,[1] T. Kobayashi,[2] M. Suzuki,[2] K. Abe,[2] K. Asai,[2] and J. Akimitsu[1]
[1]*Department of Physics and Mathematics, Aoyama-Gakuin University, Kanagawa 229-8558, Japan*
[2]*Department of Applied Physics and Chemistry, The University of Electro-Communications, Tokyo 182-8585, Japan*
(Received 4 April 2008; revised manuscript received 25 July 2008; published 27 October 2008)

We have measured the longitudinal and transverse sound velocities of $La_{2-x}Ca_xCoO_4$ $(0.4 \leq x \leq 0.7)$ propagating along [100], [110], and [001] from 200 K down to 3 K with a frequency of 10 MHz. It was found that c_{66} shows a remarkable softening below Co^{2+} spin-ordering temperature T_N in the whole doping range, while $\frac{c_{11}-c_{12}}{2}$ exhibits a clear hardening below Co^{3+} spin-ordering temperature T_{N2} only when $x=0.5$. To explain the observed anomaly, the Landau free energy for the $La_{2-x}Ca_xCoO_4$ system has been constructed, including the coupling energy between elastic strains and a two-dimensional order parameter (Q_1, Q_2), having a spatial modulation along [110] or $[\bar{1}10]$. We argued that this represents orbital order, and it is this order that leads to the softening of c_{66}.

DOI: 10.1103/PhysRevB.78.144108 PACS number(s): 62.20.de, 75.25.+z, 71.27.+a

I. INTRODUCTION

Co oxides have been an attractive subject since the report of magnetoresistivity ratios of 30% in the oxygen-deficient perovskite $RBaCo_2O_{5.4}$ (Ref. 1) and the discovery of superconductivity in the layered compound $Na_xCoO_2 \cdot yH_2O$, $x=0.35$ and $y=1.3$.[2] For $LaCoO_3$ with the perovskite structure, the origin of two magnetic anomalies observed around $T_1=100$ K and $T_2=500$ K has been argued for many years.[3–8] To interpret these anomalies consistently, several groups proposed two spin-state transitions: one is from the low spin (LS) $(S=0)$ to an intermediate spin (IS) $(S=1)$ around T_1 and the second from IS to a mix of IS and the high spin (HS) $(S=2)$ around T_2.[8,9] This model successfully explains the average magnetic moment and the lattice properties in a wide temperature range covering the two transitions. Moreover, Korotin *et al.*[9] calculated the electronic structure in the local-density approximation LDA+U approach and revealed that the energy of IS is slightly above that of LS. The octahedrally coordinated Co^{3+} ion in the IS state has an orbital degree of freedom, and orbital order may occur to lift the degeneracy of the partially filled e_g orbitals. Actually, Maris *et al.*[10] found a trace of orbital order in their x-ray diffraction studies.

$La_{2-x}Sr_xCoO_4$ has also been extensively studied for the hole-doping dependence of the spin-state transition. Moritomo *et al.*[11] observed significant reductions in resistivity and effective moment with increasing x. These changes can be ascribed to a transition of the spin state of the Co^{3+} ions from HS $(x \leq 0.6)$ to IS $(x \geq 0.8)$. The Co^{3+}(IS) state is stabilized by the double-exchange interaction between Co^{2+}(HS) and Co^{3+}(IS) ions. Co^{3+}(IS) of $La_{2-x}Sr_xCoO_4$ is expected to strongly couple with the lattice, because in $LaCoO_3$ it plays an important role in the anomalies in thermal lattice expansion[8] and elastic properties[12] relevant to the spin-state transition. Moreover, Zaliznyak *et al.*[13] discussed a possible charge glass phase with a loosely correlated checkerboard arrangement of empty and occupied $d_{3z^2-r^2}$ orbitals of Co^{3+} and Co^{2+} ions. Thus, it is of importance to clarify the elastic properties and orbital order in a layered cobalt oxide system. However, there has been no report on these properties by inelastic neutron-scattering or ultrasound measurements because of difficulties in growing large single crystals.

We have succeeded in growing large single crystals of the $La_{2-x}Ca_xCoO_4$ system, which makes it possible to carry out ultrasound measurements. The system is also a good candidate for studying the relation between elastic and magnetic properties because of its well-characterized magnetic properties. A significant reduction in the asymptotic paramagnetic Curie-Weiss temperature Θ (<0) was found by increasing x beyond about 0.7 accompanied by a reduction in μ_{eff} from $4.0\mu_B$ to $3.0\mu_B$.[14] These changes can be ascribed to a transition from Co^{3+}(HS, $x \leq 0.5$) to Co^{3+}(IS, $x \geq 0.7$) and resemble those of $La_{2-x}Sr_xCoO_4$.

Moreover, we have determined the spin and charge configuration by neutron-diffraction measurements.[15,16] A checkerboard charge order on Co^{2+}/Co^{3+} is present at room temperature, and the diffraction patterns can be indexed tetragonally $(I4/mmm)$ down to the lowest temperature. The Co-ions' spin is ordered below about 50 K. Magnetic scattering either at $q_m=(\frac{2m+1}{2}, 0, \frac{n}{2})$ or at $(\frac{2m+1}{2}, 0, n)$ was found to take place, where m and n are integers. This scattering is attributed to Co^{2+} spin order and can be explained by the difference in stacking pattern of the spin along the c axis. The correlation length of Co^{2+} spin is finite even at the lowest temperature. It should be emphasized that the correlation is significantly larger in the CoO_2 plane (the c plane) compared with the c axis. Only in $La_{1.5}Ca_{0.5}CoO_4$ we did observe the scattering due to Co^{3+} spin order at $q_m=(\frac{2m+1}{4}, \frac{2m+1}{4}, \frac{n}{2})$.

In this paper, we report on the elastic properties of $La_{2-x}Ca_xCoO_4$ $(0.4 \leq x \leq 0.7)$ of single-crystal specimens from 200 K down to 3 K. The experimental procedure and results are described in Secs. II and III. In Sec. IV, the softening of c_{66} is analyzed by the Landau theory of phase transitions. The softening is well explained by adopting a spatially modulated order parameter with a two-dimensional irreducible representation. Finally, the origin of the order parameter is discussed. Conclusions are given in Sec. V.

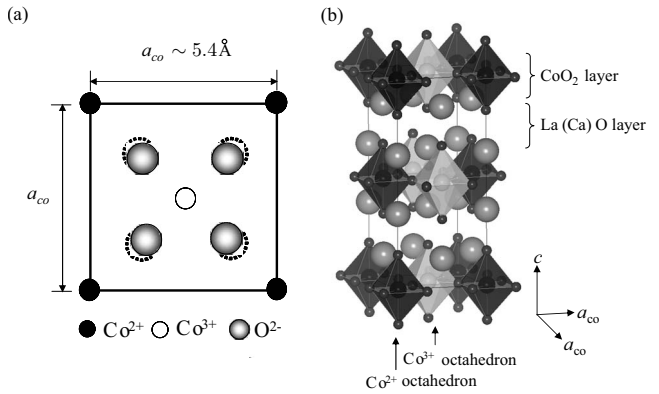

FIG. 1. (a) Checkerboardlike Co^{2+}/Co^{3+} charge configuration in the CoO_2 plane (the c plane). (b) Crystal structure of the charge ordered phase.

II. EXPERIMENTAL PROCEDURE

All polycrystalline samples were prepared by the solid-state reaction. A stoichiometric mixture of La_2O_3, $CaCO_3$, and CoO powders was sintered three times at 1200 °C for 24 h in a N_2 atmosphere. The powder x-ray diffraction measurements indicated that the powder was singly phased. Then, it was pressed into a rod 6 mm $\phi \times 100$ mm in size and sintered again at 1100 °C for 24 h. Single crystals of $La_{2-x}Ca_xCoO_4$ $(0.4 \leq x \leq 0.7)$ were grown by the floating-zone method at a feeding speed of 3 mm/h in air. Large single crystals, typically 4 mm in diameter and 70 mm in length, were obtained. The crystals were checked by a Laue photograph. They were cut by a diamond saw after alignment by Laue diffraction. The $3 \times 3 \times 3$ mm^3 specimens were subjected to ultrasound measurements. The pairs of surfaces were polished using a stainless-steel jig to maintain the crystal orientation.

Below room temperature, the crystal has a checkerboard charge order on Co^{2+}/Co^{3+}. In this paper we use a unit cell with dimensions $a_{co} \times a_{co} \times c$, as shown in Fig. 1. (At room temperature, $a_{co} \sim 5.418$ Å and $c \sim 12.47$ Å for $x=0.5$.)

The velocities of the ultrasound propagating along [110], [001], and [100] were measured by a pulse-echo method with a frequency of 10 MHz for longitudinal and transverse sounds. The absolute value was obtained from the travel time of the sound through the specimen, and the velocity change with temperature was obtained by a phase-sensitive-detection technique. For producing and detecting the ultrasound, $LiNbO_3$ transducers were bonded on both sides of the specimens with silicone adhesive for the measurements from 200 K down to 3 K. The misalignment of the polarization for transverse sound is less than 2°.

III. RESULTS

The temperature dependence of the sound velocities propagating along the principal axes of tetragonal $La_{1.5}Ca_{0.5}CoO_4$ is shown in Fig. 2, where the propagation and the polarization vectors for each sound are denoted by $\vec{k}$ and $\vec{p}$, respectively. The longitudinal and transverse sound velocities range from 4500 to 5000 m/s and 2700 to 3300 m/s, respectively, at the lowest temperature. The sound velocity v in a solid is related to the effective elastic constant c_{eff} as $v=\sqrt{c_{\text{eff}}/\rho}$, where ρ is the mass density. c_{eff}, for the measured sounds, is listed in Table I. In the temperature dependence of the velocities, we observed anomalies below about 50 K for one longitudinal sound $(\vec{k}\|\vec{p}\|[110])$ and two transverse sounds $(\vec{k}\|[100], \vec{p}\|[010])$ and $(\vec{k}\|[110], \vec{p}\|[1\bar{1}0])$. For the former two sounds with $c_{\text{eff}}=\frac{c_{11}+c_{12}+2c_{66}}{2}$ and c_{66}, the velocity decreased pronouncedly on cooling below about 50 K, while for the last sound $\frac{c_{11}-c_{12}}{2}$, the velocity increased only slightly on cooling. No anomaly was observed for the other sounds. Examination of Table I showed that both c_{66} and c_{12} decreased below about 50 K but that the softening of c_{66} was much greater in magnitude than that of c_{12}.

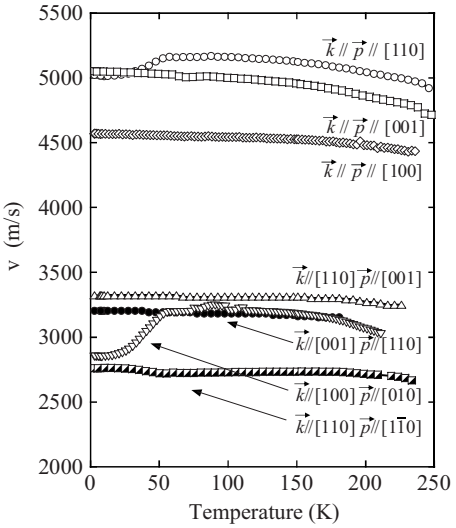

FIG. 2. Temperature dependence of the sound velocities propagating along the principal axes in $La_{1.5}Ca_{0.5}CoO_4$. $\vec{k}$ and $\vec{p}$ represent the propagation and polarization vectors, respectively.

Figure 3 shows the temperature dependence of the sound velocity for $\vec{k}\|[110]$ and $\vec{p}\|[110]$ in $La_{2-x}Ca_xCoO_4$ with $0.4 \leq x \leq 0.7$. The temperature dependence of $\frac{c_{11}+c_{12}+2c_{66}}{2}$ arises almost wholly from that of c_{66}. The observations can be summarized as follows: (1) An anomalous softening of c_{66} around 50 K in cooling is apparent throughout the doping

TABLE I. Effective elastic constants c_{eff} for the sound with the propagation vector $\vec{k}$ and the polarization vector $\vec{p}$ under tetragonal symmetry.

$\vec{k}\|$	$\vec{p}\|$	c_{eff}
[110]	[110]	$(c_{11}+c_{12}+2c_{66})/2$
[110]	[001]	c_{44}
[110]	[1$\bar{1}$0]	$(c_{11}-c_{12})/2$
[001]	[001]	c_{33}
[001]	[110]	c_{44}
[100]	[100]	c_{11}
[100]	[010]	c_{66}

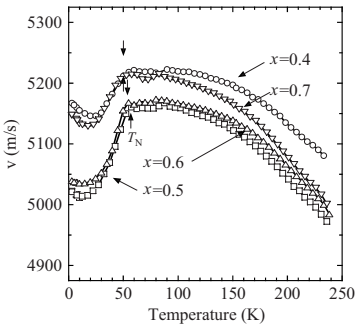

FIG. 3. Temperature dependence of the sound velocity of the longitudinal ultrasound with $\vec{k}\|[110]$ and $\vec{p}\|[110]$ for various Ca dopings. The velocity is related to $\frac{c_{11}+c_{12}+2c_{66}}{2}$. Arrows denote Co^{2+} spin-ordering temperature T_N.

range. (2) The magnitude of the softening is largest at $x=0.5$, but its x dependence is minimal. (3) For all the specimens, the onset temperature of the softening coincides with Co^{2+} spin-ordering temperature T_N determined by neutron-diffraction measurements. These results indicate that the strain relevant to c_{66} is strongly coupled to the magnetic order of Co^{2+} spins.

Figure 4 shows the temperature dependence of the sound velocity for $\vec{k}\|[110]$ and $\vec{p}\|[1\bar{1}0]$ in $La_{2-x}Ca_xCoO_4$ with $0.4 \leq x \leq 0.7$. For $x=0.5$, $\frac{c_{11}-c_{12}}{2}$ increases in cooling below about 50 K. The increment of $\frac{c_{11}-c_{12}}{2}$ becomes very small, or nonexistent, for specimens with $x \neq 0.5$. Contrary to the case of c_{66}, this anomalous hardening of $\frac{c_{11}-c_{12}}{2}$ appears only in the specimen with $x=0.5$ and is considered not to be coupled with the Co^{2+} spin order.

We now compare the anomaly observed in the present experiments with magnetic neutron scattering. Figure 5(a) shows the temperature dependence of c_{66} in $La_{1.5}Ca_{0.5}CoO_4$ obtained from the sound velocity with $\vec{k}\|[100]$ and $\vec{p}\|[010]$. The attenuation coefficient α is also shown. c_{66} starts to decrease at $T_N=53$ K in cooling and saturates at the lowest temperature. α is large in the temperature region where the temperature dependence of c_{66} is pronounced. We evaluate the anomalous part of c_{66}, Δc_{66}, as the difference between the observed c_{66} and the extrapolated one from high temperatures above T_N. The temperature dependence of $-\Delta c_{66}$ and

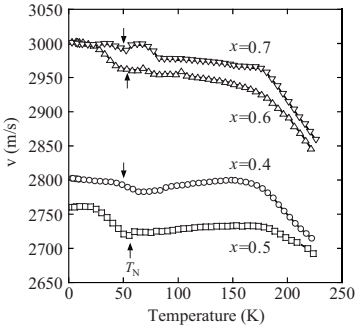

FIG. 4. Temperature dependence of the sound velocity of the transverse ultrasound with $\vec{k}\|[110]$ and $\vec{p}\|[1\bar{1}0]$. The velocity is related to $\frac{c_{11}-c_{12}}{2}$. Arrows denote Co^{2+} spin-ordering temperature T_N.

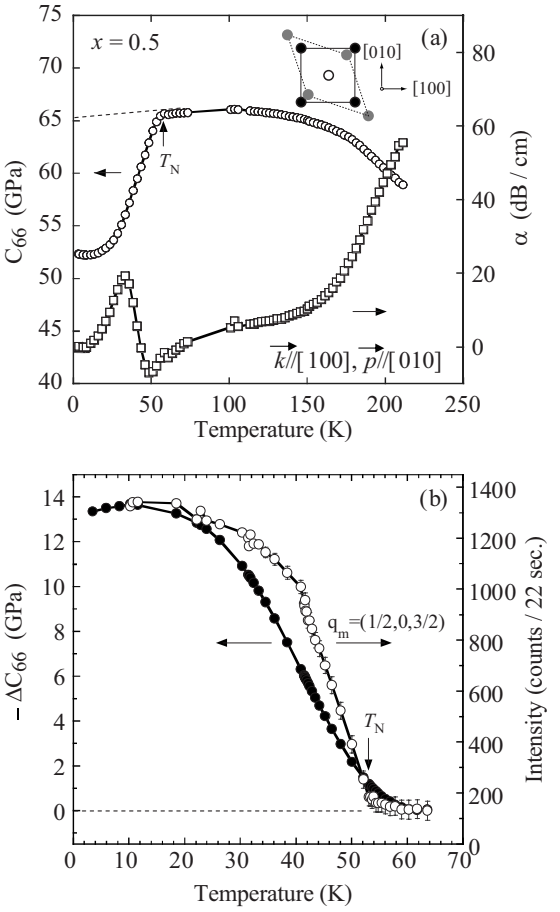

FIG. 5. (a) Temperature dependence of the elastic constant c_{66} and attenuation coefficient α for the transverse ultrasound with $\vec{k}\|[100]$ and $\vec{p}\|[010]$ in $La_{1.5}Ca_{0.5}CoO_4$. Inset: Strain relevant to c_{66}. (b) Temperature dependence of $-\Delta c_{66}$ and magnetic neutron-scattering intensity at $q_m=(\frac{1}{2},0,\frac{3}{2})$.

the magnetic scattering intensity at $q_m=(\frac{1}{2},0,\frac{3}{2})$ are shown in Fig. 5(b). The onset temperature of $-\Delta c_{66}$ is found to be very close to that of the magnetic scattering due to Co^{2+} spin order, which indicates again that the strain relevant to c_{66} is strongly correlated with this order.

Figure 6(a) shows the temperature dependence of $\frac{c_{11}-c_{12}}{2}$ in $La_{1.5}Ca_{0.5}CoO_4$ obtained from the sound velocity with $\vec{k}\|[110]$ and $\vec{p}\|[1\bar{1}0]$, together with the attenuation coefficient α. Below about 50 K, $\frac{c_{11}-c_{12}}{2}$ increases sharply during cooling and α has a broad peak around the temperature region where the temperature dependence of $\frac{c_{11}-c_{12}}{2}$ is most pronounced. The anomalous part of $\frac{c_{11}-c_{12}}{2}$, $\Delta\frac{c_{11}-c_{12}}{2}$, is evaluated as the difference between the observed and the extrapolated values from high temperatures. The temperature dependence of $\Delta\frac{c_{11}-c_{12}}{2}$ and the magnetic neutron-scattering intensity at $q_m=(\frac{1}{4},\frac{1}{4},\frac{3}{2})$ associated with Co^{3+} spin order are shown in Fig. 6(b), and temperature dependence of the two quantities is evidently similar. Co^{3+} spin-ordering temperature $T_{N2}=50$ K is close to that of Co^{2+} spin order, $T_N=53$ K, but clearly lower by a few degrees. It should be noted that both quantities, $\Delta\frac{c_{11}-c_{12}}{2}$ and the magnetic neutron-

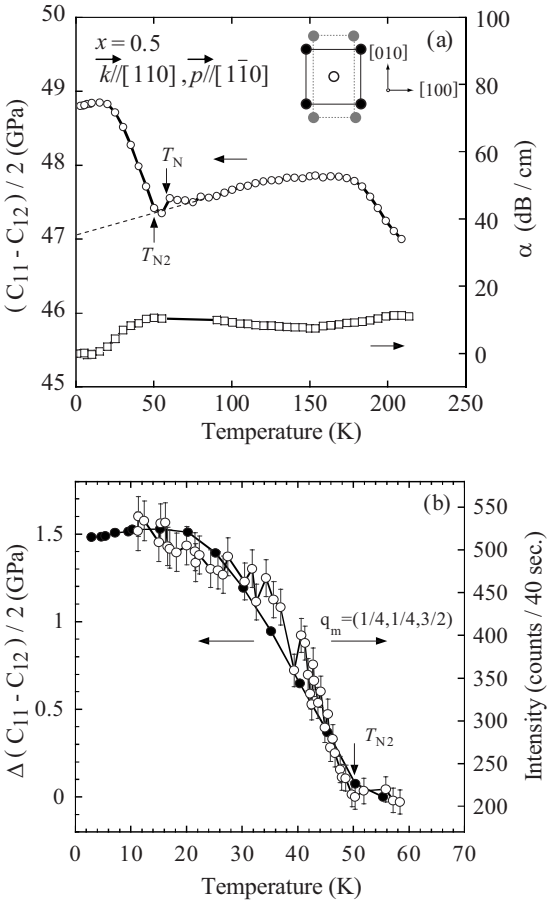

FIG. 6. (a) Temperature dependence of the elastic constant $\frac{c_{11}-c_{12}}{2}$ and attenuation coefficient α for the transverse ultrasound with $\vec{k}\|[110]$ and $\vec{p}\|[1\bar{1}0]$ in $La_{1.5}Ca_{0.5}CoO_4$. Inset: Strain relevant to $\frac{c_{11}-c_{12}}{2}$. (b) Temperature dependence of $\Delta\frac{c_{11}-c_{12}}{2}$ and magnetic neutron-scattering intensity at $q_m=(\frac{1}{4},\frac{1}{4},\frac{3}{2})$.

scattering intensity at $q_m=(\frac{1}{4},\frac{1}{4},\frac{n}{2})$, were observed only when $x=0.5$.

IV. DISCUSSION

We discuss the relationship between the anomaly of elastic constants and the magnetic order based on the Landau theory of phase transitions. Brill *et al.*[17] observed a large softening of c_{66} in $LaNiO_{4-x}$ accompanied by a structural transition attributed to a tilting of the NiO_6 octahedra. They explained the transition using Landau theory with a soft-mode phonon as the order parameter. A similar softening of c_{66} was observed in a cuprate system.[18] On the contrary, in the present system, the softening of c_{66} is strongly correlated with Co^{2+} spin order, while the change in crystal structure below T_N is minimal. This suggests that the mechanism of softening is different from the above-mentioned compounds.

To construct the Landau free energy, it should be noted that the softening of c_{66} starts at Co^{2+} spin-ordering temperature T_N and no anomaly exists above that. This feature means that the strain relevant to c_{66} is *not* the intrinsic order parameter. In addition, the following points are taken into account:

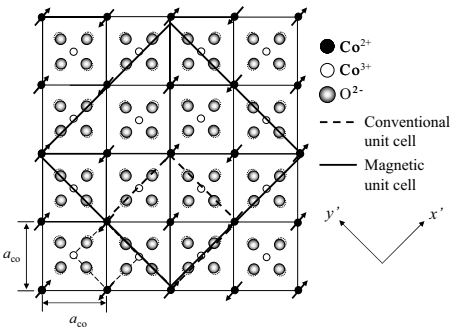

FIG. 7. Schematic spin and charge configuration of CoO_2 plane. Conventional and magnetic unit cells represent the broken and solid lines, respectively. Spin structure of Co^{3+} is only realized in $x=0.5$.

(1) The crystal symmetry in the high-temperature region is tetragonal. (Even at $x=0.5$, the distortion from tetragonal symmetry is very small.[19,20]) (2) The Co^{2+} spin configuration of the CoO_2 plane below T_N, as shown in Fig. 7, has been proved.[16]

The tetragonal symmetry of the crystal requires the order parameter to be a two-dimensional irreducible representation. Here, we choose a conventional unit cell in the paramagnetic phase with dimensions $\sqrt{2}a_{co}\times\sqrt{2}a_{co}\times c$ (D_{4h}^1-P4/mmm) and define the [110] and $[\bar{1}10]$ directions as the x' and y' axes, respectively. This cell is twice as large as the charge ordered one, and the magnetic unit cell below T_N is four times as large as this cell. Then, one finds the two-dimensional representation at the $M(\frac{1}{2},\frac{1}{2},0)$, $Z(0,0,\frac{1}{2})$, and $A(\frac{1}{2},\frac{1}{2},\frac{1}{2})$ points in the Brillouin zone of this cell.

As seen in Fig. 7, the magnetic structure is such that the Co^{2+} spins below T_N modulate transversely along the y' direction with a wavelength $\lambda=2\sqrt{2}a_{co}$. We can then adopt a spatially modulated order parameter with the two-dimensional representation

$$Q_1 = Q_{10}\exp\left(i\pi\frac{x'}{\sqrt{2}a_{co}}\right), \tag{1}$$

$$Q_2 = Q_{20}\exp\left(i\pi\frac{y'}{\sqrt{2}a_{co}}\right). \tag{2}$$

This order parameter (Q_1,Q_2) is a reasonable measure of the Co^{2+} spin configuration of the CoO_2 plane. We consider coupling between this order parameter and the lattice strain. The order parameter belongs to the E_u irreducible representation of the point group D_{4h}, while the shear strains of CoO_2 plane, $u_1=e_{x'y'}$ and $u_2=e_{x'x'}-e_{y'y'}$, to B_{2g} and B_{1g}, respectively. The lowest-order coupling terms are $u_1Q_1Q_2^*$+c.c. and $u_2(Q_1Q_1^*-Q_2Q_2^*)$. Thus, the free energy F up to the fourth order in (Q_1,Q_2) is

$$F = F_0 + \frac{\alpha}{2}(Q_{10}^2+Q_{20}^2) + \frac{\beta}{4}(Q_{10}^4+Q_{20}^4) + \frac{\gamma}{2}Q_{10}^2Q_{20}^2 + \zeta_1u_1Q_{10}Q_{20} + \frac{1}{2}\zeta_2u_2(Q_{10}^2-Q_{20}^2) + \frac{1}{2}c_1^{(\mathrm{para})}u_1^2 + \frac{1}{2}c_2^{(\mathrm{para})}u_2^2, \tag{3}$$

where $\alpha=A(T-T_N)$ and β and γ are the expansion coefficients. For stability of the system, $\beta>0$ and $\beta+\gamma>0$. $c_1^{(\mathrm{para})}$ and $c_2^{(\mathrm{para})}$ are the elastic constants in the paramagnetic phase, which correspond to $\frac{c_{11}-c_{12}}{2}$ and c_{66}, respectively.

From the minimization of F in Eq. (3) in terms of Q_{10} and Q_{20}, three sets of stable solutions are obtained. The paramagnetic phase corresponds to case I as $Q_{10}=Q_{20}=0$. On the other hand, there exist two cases for the ordered phase:

$$\text{Case II:} \quad Q_{10} \neq 0, \quad Q_{20}=0 \quad \text{or} \quad Q_{10}=0, \quad Q_{20} \neq 0.$$

$$\text{Case III:} \quad Q_{10}=Q_{20} \neq 0 \quad \text{or} \quad Q_{10}=-Q_{20} \neq 0.$$

Case II means the Co^{2+} spins modulate along the x' or y' direction, while in case III they modulate along the [010] or [100] direction. The ordered phase which takes place below T_N is selected by the inequality of the coefficients ζ_1 and ζ_2. In case II the coupling term $u_2(Q_{10}^2-Q_{20}^2)$ remains and c_{66} shows an anomaly in the ordered phase, while in case III $u_1Q_{10}Q_{20}$ instead of $\frac{c_{11}-c_{12}}{2}$ shows the anomaly.

As compared to the spin configuration shown in Fig. 7, case II is realized. Thus, the elastic constant c_{66} should be identified as

$$c_{66}=c_2^{(\mathrm{para})} \quad (T>T_N),$$

$$c_{66}=c_2^{(\mathrm{para})}-\frac{\zeta_2^2}{\beta} \quad (T<T_N). \tag{4}$$

c_{66} is constant in the paramagnetic phase and decreases stepwise at T_N. (Recall that $\beta>0$ for the stability of the system.) The observed c_{66} decreases rather gradually in a finite temperature region below T_N with a large attenuation coefficient α as shown in Fig. 5(a). This behavior can be explained by the Landau-Khalatnikov mechanism.[21] Since the frequency dependence of c_{66} has not been measured in the present experiments, in this paper we will not discuss further the deviation from the phenomenological theory for the temperature behavior of c_{66}.

Next, we consider the case of $x=0.5$, where $\frac{c_{11}-c_{12}}{2}$ shows a small hardening below T_{N2} together with a large softening of c_{66}. We cannot explain the softening of c_{66} accompanied by the hardening of $\frac{c_{11}-c_{12}}{2}$ under the tetragonal symmetry because case II and case III cannot occur simultaneously. In fact, the crystal structure of the specimen with $x=0.5$ is slightly deformed from tetragonal to orthorhombic symmetry at room temperature.[19,20] In this case, the two-dimensional representation is divided into *two* one-dimensional irreducible representations, which allows both a softening of c_{66} and a hardening of $\frac{c_{11}-c_{12}}{2}$ with different transition temperatures. It is interesting that both the hardening of $\frac{c_{11}-c_{12}}{2}$ and the magnetic scattering due to Co^{3+} spin order appear only when $x=0.5$.

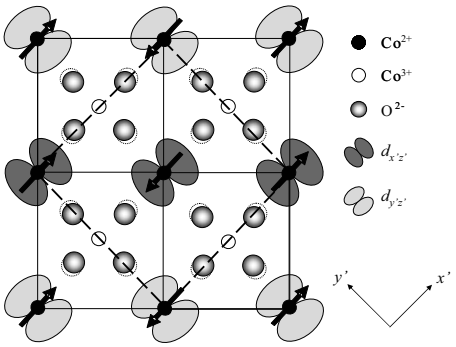

FIG. 8. Charge and spin configuration with zigzag orbital order. The broken line represents a conventional unit cell. The orbital order modulation along the [110] or [$\bar{1}$10] direction can also be regarded as an order parameter.

Finally, we discuss the order parameter (Q_1,Q_2). Spin order itself is a plausible order parameter. However, magnetostriction due at the spin ordering cannot explain the observed huge softening of c_{66}.[22] In other words, it is more appropriate to consider another quantity as a hidden order parameter causing the spin order and coupling strongly with c_{66} in the present system.

In general, spin order is strongly coupled with orbital order.[23] In fact, in t_{2g} systems such as $LaVO_3$ (Refs. 24 and 25) and other compounds,[26,27] orbital order occurs in the vicinity of the magnetic transition temperature. The orbital ordering temperature T_{oo} can be the same as the magnetic ordering temperature in the present system. We propose an orbital order in which the $d_{x'z'}$ and $d_{y'z'}$ orbitals of Co^{2+} ion are occupied alternatively in the CoO_2 plane, while $d_{x'y'}$ is occupied. The set of the $d_{x'z'}$ and $d_{y'z'}$ orbitals belongs to the E_u symmetry representation. From the direct product $E_u \times E_u=A_{1g}+A_{2g}+B_{1g}+B_{2g}$, we obtain the B_{1g} representation. Therefore, the proposed orbital order as the hidden order parameter naturally couples with the strain relevant to c_{66}. Based on this consideration, a charge and spin configuration with the zigzag orbital order is shown in Fig. 8, which is similar to the Jahn-Teller orbital order of e_g orbitals in $La_{0.5}Sr_{1.5}MnO_4$. The orbital order has the spatial modulation described by Eqs. (1) and (2).

V. CONCLUSION

We have investigated ultrasound propagating along [100], [110], and [001] of $La_{2-x}Ca_xCoO_4$ $(0.4 \leq x \leq 0.7)$. A giant softening of c_{66} was observed below T_N throughout the doping range, which is well explained based on the Landau free energy constructed from a spatially modulated order parameter (Q_1,Q_2) for tetragonal symmetry. For $x=0.5$, the coexistence of the hardening of $\frac{c_{11}-c_{12}}{2}$ below T_{N2} and the softening of c_{66} below T_N can be understood by lowering of the symmetry from tetragonal to orthorhombic. We propose that a zigzaglike orbital order from the $d_{y'z'}$ and $d_{z'x'}$ orbitals of Co^{2+} ion is realized below T_N. The proposed orbital order naturally explains the softening of c_{66}.

ACKNOWLEDGMENTS

This work was partly supported by the Iwanami Fujukai Foundation and the 21st COE program "High-Tech Research Center" Project for Private Universities: matching fund subsidy from MEXT (Ministry of Education, Culture, Sports, Science and Technology; 2002–2004) and a Grant-in-Aid for Scientific Research on Priority Areas from the Ministry of Education, Culture, Sports, Science and Technology of Japan.

[1] C. Martin, A. Maignan, D. Pelloquin, N. Nguyen, and B. Raveau, Appl. Phys. Lett. **71**, 1421 (1997).
[2] K. Takada, H. Sakurai, E. Takayama-Muromachi, F. Izumi, R. Dilanian, and T. Sasaki, Nature (London) **422**, 53 (2003).
[3] R. R. Heikes, R. C. Miller, and R. Mazelsky, Physica (Amsterdam) **30**, 1600 (1964).
[4] P. M. Raccah and J. B. Goodenough, Phys. Rev. **155**, 932 (1967).
[5] K. Asai, P. Gehring, H. Chou, and G. Shirane, Phys. Rev. B **40**, 10982 (1989).
[6] K. Asai, O. Yokokura, N. Nishimori, H. Chou, J. M. Tranquada, G. Shirane, S. Higuchi, Y. Okajima, and K. Kohn, Phys. Rev. B **50**, 3025 (1994).
[7] K. Asai, O. Yokokura, M. Suzuki, T. Naka, T. Matsumoto, H. Takahashi, N. Mori, and K. Kohn, J. Phys. Soc. Jpn. **66**, 967 (1997).
[8] K. Asai, A. Yoneda, O. Yokokura, J. M. Tranquada, G. Shirane, and K. Kohn, J. Phys. Soc. Jpn. **67**, 290 (1998).
[9] M. A. Korotin, S. Y. Ezhov, I. V. Solovyev, V. I. Anisimov, D. I. Khomskii, and G. A. Sawatzky, Phys. Rev. B **54**, 5309 (1996).
[10] G. Maris, Y. Ren, V. Volotchaev, C. Zobel, T. Lorenz, and T. T. M. Palstra, Phys. Rev. B **67**, 224423 (2003).
[11] Y. Moritomo, K. Higashi, K. Matsuda, and A. Nakamura, Phys. Rev. B **55**, R14725 (1997).
[12] T. S. Naing, T. Kobayashi, Y. Kobayashi, M. Suzuki, and K. Asai, J. Phys. Soc. Jpn. **75**, 084601 (2006).
[13] I. A. Zaliznyak, J. P. Hill, J. M. Tranquada, R. Erwin, and Y. Moritomo, Phys. Rev. Lett. **85**, 4353 (2000).
[14] K. Horigane, T. Uchida, and J. Akimitsu, Physica B **378-380**, 334 (2006).
[15] K. Horigane, K. Yamada, H. Hiraka, and J. Akimitsu, J. Magn. Magn. Mater. **310**, 774 (2007).
[16] K. Horigane, H. Hiraka, T. Uchida, K. Yamada, and J. Akimitsu, J. Phys. Soc. Jpn. **76**, 114715 (2007).
[17] T. M. Brill, G. Hampel, F. Mertens, R. Schurmann, W. Assmus, and B. Luthi, Phys. Rev. B **43**, 10548 (1991).
[18] A. Migliori, William M. Visscher, S. Wong, S. E. Brown, I. Tanaka, H. Kojima, and P. B. Allen, Phys. Rev. Lett. **64**, 2458 (1990).
[19] K. Horigane, H. Nakao, Y. Kousaka, T. Murata, Y. Noda, Y. Murakami, and J. Akimitsu, J. Phys. Soc. Jpn. **77**, 044601 (2008).
[20] The orthorhombicity is expressed by $\eta=\frac{(a-b)}{(a+b)/2}$, where a and b are the lattice constants. The value of $x=0.5$ is 0.26%.
[21] A. Bachellerie, J. Joffrin, and A. Levelut, Phys. Rev. Lett. **30**, 617 (1973).
[22] R. L. Melcher and D. I. Bolef, Phys. Rev. **186**, 491 (1969).
[23] S. Inagaki, J. Phys. Soc. Jpn. **39**, 596 (1975).
[24] H. Sawada and K. Terakura, Phys. Rev. B **58**, 6831 (1998).
[25] M. Noguchi, A. Nakazawa, S. Oka, T. Arima, Y. Wakabayashi, H. Nakao, and Y. Murakami, Phys. Rev. B **62**, R9271 (2000).
[26] W. Jauch and M. Reehuis, Phys. Rev. B **65**, 125111 (2002).
[27] J. Hemberger, H. A. Krug von Nidda, V. Fritsch, J. Deisenhofer, S. Lobina, T. Rudolf, P. Lunkenheimer, F. Lichtenberg, A. Loidl, D. Bruns, and B. Buchner, Phys. Rev. Lett. **91**, 066403 (2003).